IVYSPRING INTERNATIONAL PUBLISHER

International Journal of Biological Sciences

2027; 23(1): 358-375. doi: 10.7150/ijbs.142563

Research Paper

Personalized Colorectal Cancer Therapy Guided by Patient-Derived Organoids for Different Gene Mutations

Jinghong Chen[1,2,3#], Jing-Bo Zhou[1,4#], Fangyuan Shao[1,2#✉], Yangyang Feng[1], Xiangpeng Chu[1], Ling Li[1], Kai Miao[1,2], Duo Liu[5,6], Weihao Deng[6], Wen-Li Zhu[7], Guang-Hui Luo[7], Kin-Iong Chan[7], Zheyu Cai[3], Jinbao Liu[3], Jian Cai[5,6✉], Chu-Xia Deng[1,2,8✉]

1. Faculty of Health Sciences, University of Macau, Macau SAR, China.
2. MoE Frontiers Science Center for Precision Oncology, University of Macau, Macau SAR, China.
3. Laboratory Animal Center, Guangzhou Municipal and Guangdong Provincial Key Laboratory of Protein Modification and Degradation, School of Basic Medical Sciences, Guangzhou Medical University, Guangzhou, China.
4. Guangdong Key Laboratory of New Technology in Rice Breeding, Rice Research Institute, Guangdong Academy of Agricultural Sciences, Guangzhou, China.
5. Department of Colorectal Surgery, Shenzhen Second People's Hospital, Health Science Center, Shenzhen University, Shenzhen, China.
6. Department of Colorectal Surgery, Department of General Surgery, Guangdong Institute of Gastroenterology, Guangdong Provincial Key Laboratory of Colorectal and Pelvic Floor Diseases, The Sixth Affiliated Hospital, Sun Yat-Sen University, Guangzhou, Guangdong, China.
7. Kiang Wu Hospital, Macau SAR 999078, China.
8. Faculty of Synthetic Biology, Shenzhen University of Advanced Technology, Shenzhen 518107, China.

#These authors contributed equally.

✉ Corresponding authors: Chu-Xia Deng, Phone: E-mail: dengchuxia@suat-sz.edu.cn. Jian Cai, Phone: 86 13822182753, Fax +86 755-83003435, Email caijian_dr@email.szu.edu.cn. Fangyuan Shao, Phone: (853) 8822 2903; E-mail: fangyuanshao@um.edu.mo.

© 2027 The Author(s). This is an open access article distributed under the Creative Commons Attribution 4.0 International Licence, subject to the Publisher's Terms of Use at https://ivyspring.com/terms.

Received: 2026.08.14; Accepted: 2026.08.18; Published: 2027.01.01

Abstract

The multistep progression of colorectal cancer involves alterations of key driver genes, such as *APC*, *KRAS*, *SMAD4*, and *P53*. Precision oncology aims to predict drug responses accurately based on the molecular profiles of tumors. In this study, we performed drug screening on patient-derived colorectal organoids (PDOs) harboring various gene mutations to gain valuable insights into the pharmacogenomics of human colorectal cancer (CRC). Notably, we observed a higher prevalence of TP53 mutations in clinical stage III samples and those located in the sigmoid region. Interestingly, these mutated PDOs recapitulated the characteristics of their respective parental tumors. Additionally, our results revealed distinct drug responses depending on the specific gene mutations. We retrospectively followed 19 patients and compared their clinical responses with PDO drug screening results, which showed 76.30% accuracy and 100% sensitivity. Finally, we treated four late-stage patients with drugs suggested by PDO screening, achieving stable responses. These findings advance our understanding of the pharmacogenomics landscape influenced by molecular abnormalities and highlight the significance of phenotype-driven screening using PDOs for the development of novel treatment strategies.

Keywords: colorectal cancer, patient-derived organoids, pharmacogenomics, drug sensitivity test, clinical responses, synthetic biology

Introduction

Colorectal cancer (CRC) is the third most diagnosed cancer and the second leading cause of cancer-related death worldwide [1]. In 2022, close to 1.9 million new cases and approximately 0.9 million deaths were reported worldwide for CRC [1]. Despite advancements in screening programs and therapeutic strategies, CRC remains a significant public health challenge. The pathogenesis of CRC is characterized by a series of genetic mutations. The biallelic loss of *APC*, occurring in over 80% of cases, is frequently the

initiating or gatekeeping mutation for CRC [2, 3]. Activating mutations in Kirsten rat sarcoma (*KRAS*) are commonly observed in more advanced stages of CRC, particularly in the progression from early to intermediate adenomas [4]. Loss-of-function mutations in *SMAD4* and *TP53* occur in the intermediate to late stages of adenoma and from the late stages of adenoma to adenocarcinoma, respectively [5]. The prognosis of CRC is heterogeneous. Approximately 50-60% of patients diagnosed with CRC will develop colorectal metastases [6-9]. Patients with metastatic disease (mCRC) are increasingly treated accordingly to their tumor's underpinning molecular profile.

Next-generation sequencing (NGS) and subsequent bioinformatic analysis provide tremendous insight into the individual genomic landscape of cancer and guide treatment decisions for optimal patient outcomes [10, 11]. Insights from cancer genomics have broadened the list of gene-drug pairs, motivated clinicians to incorporate them into precision genomic medicine, facilitating the tailoring of treatment regimens per patient based on the genotype of individual tumors [12, 13]. Despite its potential, precision oncology remains a challenge, not only because of the genetic heterogeneity of human tumors, but also because of the poor responsiveness of drugs and tumors in patients [14-16]. The response to drug treatment also hinges on the molecular and phenotypic alterations that characterize human cancers and tumorigenic processes [17, 18]. Furthermore, more therapeutic drugs that can be used for the treatment of CRC are necessary.

Patient-derived tumor organoids (PDOs) are cultures of tumor cells derived from individual patients which have a high success rate, are less expensive, and grow rapidly while maintaining intra-tumoral heterogeneity [19, 20]. Studies, including those from our research group, have conducted drug screening using PDO culture system such as breast cancer, nasopharyngeal carcinoma, gastric cancer, prostate cancer, liver cancer, colorectal cancer, and pancreatic cancer, etc. [21-24]. In fact, these studies demonstrated that this system has great potential to assess patients' response to targeted therapies, chemotherapy, and radiation [6, 25, 26].

To enhance our understanding of the relationship between the PDO screening system and the mutation genes of colorectal cancer, we employed precise pharmacogenomic methods that combine the genomics of colorectal cancer's mutations with the drug sensitivity sequencing of PDO, allowing for a comprehensive study of effective treatment plans for different gene mutation types. Our research illustrates that drug screening data, conducted under various mutant backgrounds, including mutants in *APC*, *KRAS*, *SMAD4*, and *TP53*, unveil specific strategies for treating patients using a combination of drugs tailored to CRC mutation types.

Results

Patient samples and clinical information

A total of 148 colorectal cancer patients were enrolled from two hospitals in this study (**Supplemental Data file 1**), and we further studied their histological and clinical features. The patient demographics and tumor characteristics are shown in **Table 1**. All colorectal patients were of Chinese origin with a median diagnosed age of 63 years. Regarding tumor characteristics, 87.16% of tumors were of moderate differentiation grade, while 12.84% were low differentiation grade. Metastatic colorectal cancer samples were obtained from tumors in the lymph nodes (n=63), peritoneum (n=13), liver (n=9), lung (n=9), and bone (n=1). 70.95% of tumors were left-sided and 27.70% were right-sided. The colorectal tumors were subdivided into sigmoid colon, rectum cancer, transverse colon, ascending colon, and descending colon, with respective percentages of 31.08%, 29.73%,19.59%,5.41% and 6.08%. The clinical stages of tumor were divided into four stages: I (11.49), II (22.97%), III (42.57%), and IV (18.92).

Mutational landscapes of colorectal cancer

To further investigate gene-specific genomic features and therapeutic prognosis, we performed the whole-exome sequencing (WES) to study the genomic landscape of colorectal gene types. In total, we detected 50,053 somatic mutations, including 40,490 missense mutations, 3,997 deletions, 2,034 nonsense mutations, 1,394 insertion mutations, 1,311 splice site mutations, 538 in-frame deletion, 192 in-frame insertions and 289 other types of mutations from 148 patients. These results were obtained from three different mutant callers (MuTect2, Strelka2 and LANCET) (**Figure 1A, B**). The recurred mutations presented in Fig. 1A showed the oncogenic drivers of CRC, such as *APC* (mutational frequency at 64.9%), *KRAS* (33.6%), *SMAD4* (8.2%) and *TP53* (56%). This was consistent with previous research findings [27]. The most frequently mutated genes converged into signaling pathways involved in WNT signaling, cell cycle, vascular endothelial growth (VEGF), PI3K/AKT signaling, mammalian target of rapamycin (mTOR), mitogen-activated protein kinases (MAPKs), apoptosis, notch signaling, and mitosis regulation (**Figure 1A**). Among these top mutated pathways, WNT signaling (*APC*), cell cycle (*TP53*), VEGF (*KRAS*), PI3K/AKT signaling (*LAMA3*, mutational frequency

at 10.2%), mTOR (*BRAF*, 8.2%), MAPKs (*TGFBR2*, 7.5%), apoptosis (*SPTA1*, 13.4%), NOTCH (*NOTCH3*, 9.0%), and mitosis regulation (*TTN*, 38.1%) showed considerably high mutational frequencies in colorectal mutations. We further analyzed base mutations in 148 colorectal cancers. The analysis of the mutational signatures revealed that C>T base substitutions were the predominant signatures in colorectal cancers (**Figure 1C**).

The analysis of the total number of SNV mutations was conducted in relation to clinical characteristics, which included age, gender, tumor differentiation grade, tumor stage, primary tumor location, metastasis, pathological type and patient status. Significant differences were observed in tumor differentiation grade (moderately and poorly, P=0.0026), tumor stage (I, II, III, and IV, P=0.013), primary tumor location (left and right, P=0.0274), primary tumor location (sigmoid, rectum, ascending, transverse and descending, P=0.032) (**Figure 1D-G**). However, no significant distinction (p>0.05) was found with respect to age, gender (male and female), metastasis (yes or no), pathological type (adenocarcinoma and mucinous adenocarcinoma), and patient status (live and dead) (**Supplemental Figure 1A-E**).

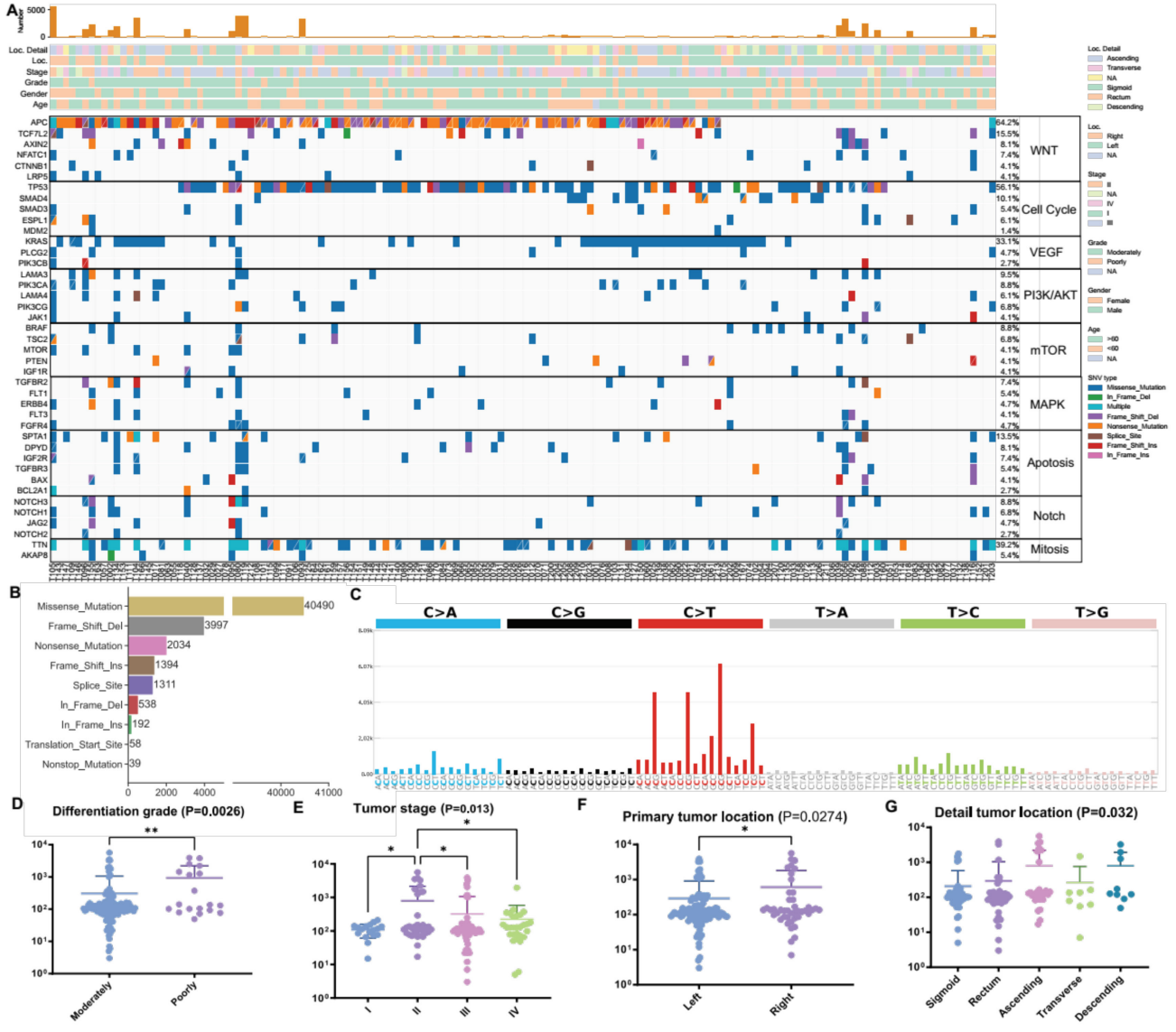


Figure 1. Histological and molecular landscape of colorectal cancer. A. Top recurrent protein coding single nucleotide variants (SNVs) identified from this cohort are represented in a pathway-wise manner, including WNT, Cell Cycle, VEGF, PI3K/AKT signaling, mTOR, MAPK, Apoptosis pathway, Notch, Mitosis regulation. SNV mutational rate for each tumor is shown at the top of the panel. Information of location detail, location, tumor stage, differentiation grade, gender, and age of diagnosis is also provided at the top of the panel. Tumor samples (n = 148) were assigned for SNV identification. **B.** Detailed somatic variation types and amounts discovered from this CRC cohort. A total of 50,053 somatic mutations included 40,490 missense mutations, 3,997 frame shift deletion, 2,034 nonsense mutations, 1,311 splice site, 1,394 frame shift insertion, 538 in frame deletion, 192 in frame insertion, 58 translation start site, and 39 nonstop mutation (n = 148 tumors) are shown. **C.** Overall mutational signature of this CRC cohort revealed C > A and C > T base substitutions are predominant mutational signature in CRC (n = 148 tumors). **D-G.** The total number of SNV mutations was analyzed in relation to clinical characteristics such as tumor 2 differentiation grade, tumor stage, primary tumor location, and detailed tumor location (P<0.05).

Table 1. Patient demographics and tumor characteristics.

Characteristic	Category	Tumor group (N = 148)	
		No.	%
Age, median (IQR), y, no. (%)	≥60	98	66.22%
	<60	49	33.11%
	N/A	1	0.70%
Gender, no. (%)	Male	77	52.03%
	Female	71	47.97%
Tumor Differentiation grade, no. (%)	Moderate	129	87.16%
	Poor	19	12.84%
Metastases, no. (%)	Yes	82	55.41%
	No	63	42.57%
	N/A	3	2.00%
Pathological type, no. (%)	Adenocarcinoma	135	91.22%
	Mucinous adenocarcinoma	13	8.78%
Patient Current status, no. (%)	Live	105	70.95%
	Dead	15	10.13%
	N/A	28	18.92%
Primary tumor location 1, n (%)	Left colon	105	70.95%
	Right colon	41	27.70%
	N/A	2	1.35%
Primary tumor location 2, n (%)	Sigmoid colon	46	31.08%
	Rectum colon	44	29.73%
	Ascending colon	29	19.59%
	Transverse colon	8	5.41%
	Descending colon	9	6.08%
	N/A	12	8.11%
Tumor Stage, n (%)	I	17	11.49%
	II	34	22.97%
	III	63	42.57%
	IV	28	18.92%
	UK	6	4.05%

AKSP mutation classification of colorectal cancer recapitulates the genetic characterization of parental tumors

To provide a more comprehensive understanding of the genes and evolutionary forces driving CRC, we categorized and analyzed our collected tumor samples based on several major mutations, i.e. *APC* (A), *KRAS* (K), *SMAD4* (S) and *TP53* (P) (AKSP) mutations. The *APC*, *SMAD4*, and *TP53* are tumor suppressor genes and their mutations involve both CNVs including deletion mutation and somatic SNVs, which include missense, frameshift deletion, frameshift insertion, nonsense, in-frame deletion and splice site mutation [28, 29]. The *KRAS* (K) mutations refer to SNV location in G12 position [28, 29].

CNVs at the gene level were called by Sequenza and CNV kit, with only consensus results from both callers retained for further analysis (**Figure 2A**). *APC* SNVs and CNVs were found in 70.95% cases (105 of 148), which included 10 deletions and 95 other mutations. *SMAD4* SNVs and CNVs were present in 60.13% cases (89 of 148), including 74 deletions and 15 other mutations. *TP53* SNVs and CNVs were observed in 70.95% cases (105 of 148), including 22 deletions and 83 other mutations. *KRAS* G12 mutations were found in 22.97% cases (34 of 148) (**Figure 2B**). **Figure 2C** displays the percentage of each genotype in 148 colorectal cancer tumors. The ASP mutated genotype had the highest mutation frequency at 35.8% (53 of 148 cases). The second most common mutated genotype was AKSP, which was found in 10.8% (16 of 148 cases). Interestingly, we discovered that 15 samples did not have CNV or SNV in AKSP, accounting for 10.1% of the cases. Furthermore, 11 samples (7.4%) had only A or P mutations. The AK or SP mutated genotype was found in 6 samples (4.1%), and the SP mutated genotype was found in 8 samples (5.4%).

We examined the total number of mutations corresponding to different gene mutated genotypes. Our findings revealed that the total number of mutations in SNVs with either AKSP or ASP mutated genotypes was more stable and lower than those with only A or P mutated genotypes (**Figure 2D**). This indicates that A or P mutated genotypes might need other genes mutated for cancer development. Significant differences were observed in the overall chromosomal gain and loss frequencies among different gene mutated subtypes (**Figure 2E**). Upon combining the clinical stage and site of tumorigenesis, we found that most samples with TP53 mutations were in clinical stage III and located at the sigmoid colon (**Supplemental Figure 2 A, B**).

Further investigation on somatic CNVs revealed that frequent chromosomal amplifications of Chr. 7, 8, 13, and deletions of 4, 14, 15, and 18 were the major features of colorectal cancer across all subtypes, which suggests that such recurrent changes were critical genetic events leading to CRC tumorigenesis. However, the somatic copy number alteration landscape was analyzed in 148 colorectal tumors classified by AKSP mutation status (**Supplemental Figure 2C–N**). AKSP and ASP showed the highest frequencies of copy-number amplifications and deletions, while K and None were the least common.

Patient-derived organoids recapitulate features of parental tumors

Previous studies have demonstrated that colorectal cancer organoids can replicate the histological characteristics of their parental tumors [30]. However, it is unclear whether this also applies to organoids treated with drugs. To investigate this, whole-exome sequencing (WES) was conducted on 39 pairs of colorectal cancer patient-derived organoids (PDOs) (passages 1–2) and their parental tumors. The aim is to ascertain whether the organoids, derived from both drug-treated and treatment-naïve tumors, retained the genomic features of the parental tumors.

The results of SNVs revealed that mutations in cancer-related genes, considered to be tumor-specific drivers, were largely preserved in the paired PDOs (**Figure 3A**). Copy number alterations (CNAs) demonstrated that DNA copy number losses and gains of parental tumors were generally retained in the colorectal cancer PDOs across the entire genome. This included PDOs derived from drug-treated and metastatic tumors (**Figure 3B**). Further investigation on tumor and organoids CNAs revealed that frequent chromosomal deletions of chromosomes 4, 5, 14, 15, and 18, along with amplifications of chromosomes 2, 7, 13, were the major features of colorectal cancer across all genotypes. In summary, paired tumors and PDOs maintained consistent mutational signature profiles.



Figure 2. AKSP mutated classification recapitulate the genetic characterization of parental tumors. A. Somatic mutations and the copy number of altered cancer genes found in CRC related genes are present and conserved in tumor. Mutation type is indicated in the legend. **B.** The percentages of *APC*, *KRAS*, *SMAD4* and *TP53* classification in each type. *APC*: mutation, 64.19% (n = 95); amplification, 28.38% (n = 42); deletion, 6.76% (n = 10); wildtype, 0.68% (n=1). *KRAS*: active mutation, 22.97% (n = 34); other mutation, 9.5 % (n = 14); amplification, 8.78% (n=13); deletion, 4.05% (n = 6); wildtype, 54.73%(n=81). *SMAD4* mutation, 10.14% (n = 15); deletion, 50% (n = 74); wildtype, 39.86% (n=59).*TP53*: mutation, 56.08% (n = 83); amplification, 2.03% (n = 3); deletion, 14.86% (n = 22); wildtype, 27.03% (n=40). **C.** The number and percentages of each type in 148 samples. **D.** The total number of SNV mutations in each type is shown. There are significant differences in four pairs of types, which are None mutation (None) with A, None with A+K type, None with A+K+S type, None with A+K+S+P type. **E.** The absolute Log2 copy ratio of CNV in each type is displayed. There are significant differences in four pairs of types, which are None with A, None with A+K type, None with A+K+S type, None with A+K+S+P type.

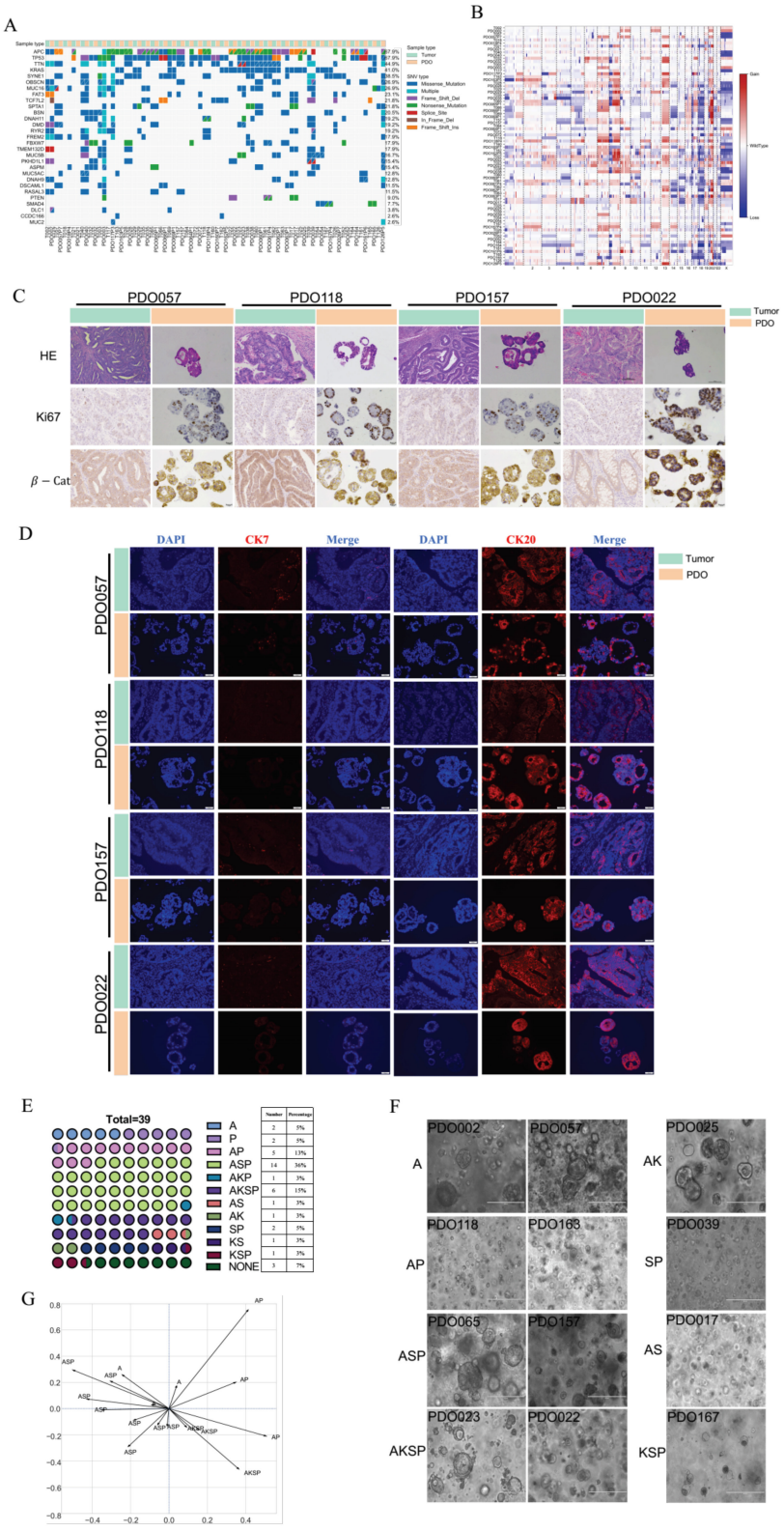


Figure 3. Recapitulation of genetic characterization of parental tumors in colorectal cancer organoids. A. Heatmap comparing the somatic mutated cancer genes in 39 pairs of colorectal cancer organoids and parental tumors. Mutation type is indicated in the legend. **B.** Comparison of the somatic copy number alteration landscape in colorectal cancer organoids with those in parental tumors. Copy number gain is shaded in red and copy number loss is shaded in blue. **C.** Histological and immunohistochemical images showing the organization structure and status of proliferation marker (Ki-67) and β-catenin in primary tumors and PDOs. Scale bar: 50 μm. Green bar means tumor tissue, and orange bar means organoids at the top. **D.** Immunofluorescence images showing the organization structure and colorectal cancerrelated markers (CK7 and CK20) in primary tumors and PDOs. Scale bar: 50 μm. Green bar means tumor tissue, and orange bar means organoids at the top. **E.** The number and percentages of each type in 39 organoids. **F.** Bright-field microscopy images showing the representative phenotypes of colorectal cancer organoids. The first column images showed A and AK mutation type organoids. The second column images showed AP and SP mutation type organoids. The third column images show ASP and AS mutation type organoids. The fourth column images showed AKSP and KSP mutation type organoids. Scale bar:100 μm. **G.** Unsupervised clustering by principal component analysis (PCA) on sample-wise PDO transcriptome. Organoids derived from the same subtypes were well clustered into the corresponding subtypes.

Histopathologic characteristics were compared in these pairs of colorectal cancer organoids (passage 1–2) and parental tumors. Haematoxylin and eosin (H&E) staining was performed to compare the morphological features of organoids and original tumors. We found that the PDOs recapitulated the histologic features of their parental tumor tissues, including growth patterns and cellular and nuclear atypia (**Figure 3C**). The tumors and matched organoids were analyzed for the presence of β-catenin and Ki-67, common biomarkers for colorectal cancer. Additionally, two other molecular markers of intestinal cancer, CK7 and CK20, were detected by immunofluorescence staining. CK7 was found to be negatively expressed in both organoid and tumor, while CK20 was positively expressed in both organoid and tumor (**Figure 3D**). The result from the immunohistochemical staining and immunofluorescence staining revealed that the expression pattern of colorectal cancer markers was well preserved in organoids derived from tumors with different mutations.

In the end, we generated 96 organoids from the 134 colorectal cancer samples, with an overall success rate of 71.64%. DNA sequencing was performed on 39 organoids and the mutations in each of the *APC*, *KRAS*, *SMAD4* and *TP53* genes and various combinations were identified (**Figure 3E**). The highest mutations occurred in ASP genes (36%, 14/39), followed by AKSP genes (15%, 6/39) and other combinations, whereas 3 organoids had mutations in none of the 4 genes (7%). These percentages of organoid mutation types are consistent with the percentages of tumor mutation types, reflecting a fact that besides these 4 genes, some other genes also play a role in colorectal cancer formation (**Supplemental Figure 4F**). Morphological observations revealed a double-layered membrane cavity structure in the colorectal organoids, consistent across different genetic mutation types.

Transcriptome sequencing was performed for 17 PDOs and then used for unsupervised clustering by principal component analysis (PCA) to assess the overall transcriptional pattern of the samples (**Figure 3G**). The results showed that organoids of the same mutation type clustered well into corresponding mutation types, and the different PDO type maintained its differences in mutation types at the transcriptional level. RNA-seq results suggest that different types of mutations exhibit different driving mechanisms, including WNT, RTK, and the cell cycle. Differentially expressed genes were filtered by DESeq2 (log2 fold change > 1, p-value < 0.05, FDR value < 0.05) and then presented in a heatmap (**Supplemental Figure 3A-C**). We conducted pathway enrichment analysis on the transcriptome sequencing results and presented them in the form of a heatmap (**Supplemental Figure 3A-C**). A comparison of pairwise mutation types shows that the highly expressed pathway of the A mutation type is DNA-damage response, FOXO3 targets, NF-kB, and the colorectal cancer pathway. The main pathways for the AKSP mutation type are PARP, PRKCA, and JAK2. Compared with AKSP mutations, AP has enriched pathways such as ribosomes, H3k4me3, Fgfr2, and tamoxifen metabolism. Another AKSP mutation type pathway is enriched as AKL, P38-MK2, TGFB. We also compared the ASP and AKSP mutation type enrichment pathways, with the ASP mutation type pathways mainly being Mir21, PI3K-FGFR, and tumor escape from immune. The AKSP mutation type pathway is apoptosis, APC, and P38-MK2. Notably, differentially expressed pathway genes were also present between A and AKSP mutation genotypes, AP and AKSP mutation genotypes, and ASP and AKSP mutation genotypes (**Supplemental Figure 3A-C**).

Drug screening with APC/KRAS/SMAD4/TP53 mutation colorectal cancer organoid

To explore personalized therapy, we conducted the drug sensitivity test for each individual PDO model from human colorectal cancer tissue. Diverging from previous organoid culture studies, we combined drug sensitivity with genomic features to establish a precision oncology pipeline for comprehensive pharmacogenomics studies. Subsequently, we carried out drug screening to identify effective therapeutic candidates using PDOs at passages 1-3 within 2-3 weeks of biopsy collection. We first studied 39 organoids on several first-line colorectal chemotherapeutic agents and the data showed that most organoids were relatively sensitive to topoisomerase inhibitors (irinotecan, doxorubicin and epirubicin hydrochloride), resistant to VEGFR inhibitors (regorafenib and sorafenib), and exhibited varying responses to DNA/RNA synthesis inhibitors (5-FU, oxaliplatin, capecitabine and leucovorin calcium pentahydrate) (**Figure 4A, B**). Of note, two organoids with mutations in *APC* gene only (A) seemed more sensitive to 5-Fu and Oxaliplatin (**Figure 4A, B**).

To further verify that different mutation genotypes respond varied to drugs, we treated resistant and sensitive organoids with 5-FU and oxaliplatin, respectively. Following 48 hours of treatment, we observed a significant reduction in both the size and number of organoids in the sensitive lines (**Figure 4C**). Conversely, the size and count of the organoids in the resistant lines remained unchanged compared to the control.

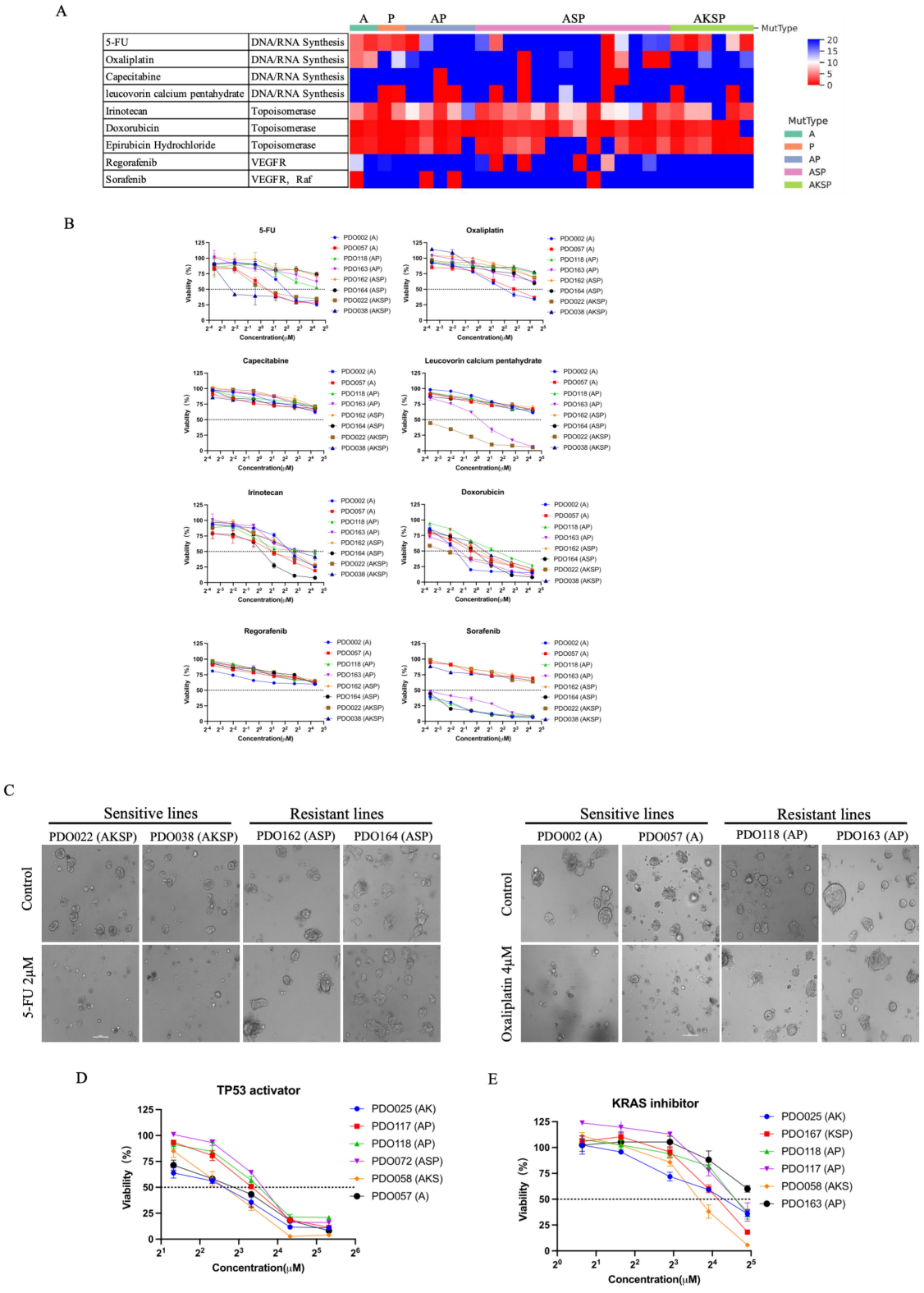


Figure 4. A/K/S/P mutation colorectal cancer organoids serve as a platform for preclinical drug screening. A. Heatmap showing the IC50 values and corresponding percentage of 9 chemotherapy drugs for colorectal cancer in 29 PDOs. They were divided into five groups according 7 to A/P/AP/ASP/AKSP mutation type at the top graph. The tested drugs and their targets are listed on the left. Dose–response graph is indicated on the right. The tested drugs are listed on the right. **B.** Representative drugs (5-FU, oxaliplatin, capecitabine, leucovorin calcium pentahydrate, irinotecan, doxorubicin, regorafenib and sorafenib) response curves for PDO002(A), PDO057(A), PDO118(AP), PDO163(AP) PDO162(ASP), PDO164(ASP), PDO022(AKSP), PDO038(AKSP). The results are expressed as the mean ± standard error of the mean (S.E.M.). **C.** Bright-field microscopy images showing the morphological differences between 5-FU-resistant (PDO022, PDO038) and -sensitive (PDO162, PDO164) organoids, oxaliplatin-resistant (PDO002, PDO057) and -sensitive (PDO118, PDO163) after 48h of treatment. Scale bar: 50μm. **D.** Nutlin3(TP53 antagonist) drug response curves for PDO025(AK), PDO058(AKS), PDO057(A), PDO117(AP) PDO118(AP), PDO072(ASP). The results are expressed as the mean ± standard error of the mean (S.E.M.). **E.** Sotorasib (KRAS G12C inhibitor) drug response curves for PDO025(AK), PDO058(AKS), PDO057(A), PDO117(AP) PDO118(AP), PDO072(ASP). The results are expressed as the mean ± standard error of the mean (S.E.M.).

Next, we extended the drug test to a drug library of 49 drugs, including 18 chemotherapy drugs (**Supplemental Figure 4A**) and 31 target drugs (**Supplemental Figure 4C, Supplemental Data file 2**). In general, none of the PDOs showed identical drug responses, reflecting individual differences, although there were subtype-specific responses to certain drugs. The data also showed that while the different mutated genotypes of PDOs were predominantly sensitive to topoisomerase, microtubule inhibitors (MTi) and EGFR targets, they exhibited varied responses to DNA/RNA synthesis targets (**Supplemental Figure 4A, C**).

Of the three MTi drugs tested, docetaxel and paclitaxel were effective against most organoids, each with four resistant lines (**Supplemental Figure 4A, B, E**). Vincristine produced good responses in organoids with A- or P-type mutations but was ineffective in most other genotypes (**Supplemental Figure 4A, B, E**). For the six EGFR-targeting drugs tested, all except lapatinib ditosylate showed good responses in most organoids, with afatinib producing the strongest effect (**Supplemental Figure 4C, D**). Drugs targeting C-Met (crizotinib), PP2A (cantharidin), and HDAC (vorinostat) all produced strong responses in these PDOs (**Supplemental Figure 4C, D).** Other organoid drug-screening results are presented in **Supplemental Figure 4E**. Some representative drug responses were replicated and were displayed in **Supplemental Figure 4G**. For gefitinib and erlotinib, most organoid mutant types showed moderate responses, except for the AP mutant organoid (PDO0118), which was sensitive to erlotinib (**Supplemental Figure 4G**).

Based on the genomic profiles of the CRC organoids, we next sought to correlate drug responses with genome-wide genetic alterations. It is known that the *TP53* mutation is found in approximately 60% of colorectal cancers. In line with this, the *TP53* mutation rate increases to 80% in patients with advanced colorectal cancer who had metastases [31]. Conversely, *TP53* mutations are infrequent in benign colonic adenomatous polyps [32], with alteration frequencies ranging between 15% and 30% [33]. Nutlin3 (Nut3), a cis-imidazoline analog, disrupts the binding between MDM2 and p53, acting as an antagonist of MDM2, an E3 ubiquitin ligase of protein of the p53 family [34]. In accordance with previous findings [30, 35, 36], all *TP53*-mutated PDOs exhibited greater resistance to nutlin-3 than the *TP53* wildtype (**Figure 4D**). Of the genes studied, *KRAS* was the least frequently mutated, affecting approximately 30% of tumors. Moreover, KRAS codon 12 mutations have been associated with advanced stages of CRC [37], and there is a high concordance of KRAS mutations between primary and metastatic CRC [38]. Subsequently, we used FDA-approved *KRAS* G12C inhibitor, sotorasib, for the treatment of colorectal PDOs. We observed that all *KRAS* G12C–mutated PDOs were more sensitive to sotorasib than *KRAS* wild-type PDOs (**Figure 4E**).

PDO pharmaco-phenotyping reflects the previous treatment responses of the corresponding patient

To determine whether pharmaco-phenotyping of PDOs could reflect drug responses of patients, we tracked 19 patient cases with clear retrospective data. T197 was obtained from a patient diagnosed with colorectal cancer with peritoneal metastasis. The patient underwent omentectomy in October 2021 and received 12 cycles of combination chemotherapy with 5-FU, irinotecan, oxaliplatin, and the anti-VEGF antibody bevacizumab from November 2021 through March 2022, achieving a partial response (PR**) (Figure 5A).** We used omental tumor tissue to generate organoids and performed drug sensitivity testing. Based on our pharmaco-phenotyping results, PDO197 showed sensitive responses to several drug combinations, including 5-FU+irinotecan +oxaliplatin **(Figure 5B),** which was used for the treatment of the patient. PDO197 was sensitive to the 5-FU+oxaliplatin and 5-FU+irinotecan combinations, showed a moderate response to sorafenib, but was resistant to 5-FU and to raltitrexed (**Figure 5C**).

Patient T199, diagnosed with colorectal cancer with pulmonary peritoneal metastasis, was treated with chemotherapy drugs (5-FU+oxaliplatin) and bevacizumab before paracentesis. Because the patient was resistant to the treatment, the drug combination was switched to 5-FU+irinotecan and bevacizumab for 8 courses from April 2021 to June 2021, which achieved a stable disease (SD). In September 2021, after the change of drug to trametinib + HCQ, the disease had changed from SD to PR (**Figure 5D, E**). We derived organoids (PDO199) from the colon tumor tissue of this patient and conducted drug screening during these treatments. Pharmaco-phenotyping results showed that PDO199 was resistant to 5-FU+oxaliplatin, which were the first drugs used for the treatment and yielded a PD, but sensitive to 5-FU+irinotecan and trametinib+HCQ, which were used later to achieve PR (**Figure 6D-F**). The PDO199 was also sensitive to some other drugs, including trametinib, bortezomib, trametinib+HCQ, trametinib+HCQ+docetaxel, docetaxel+oxaliplatin, 5-FU+ irinotecan+oxaliplatin, regorafenib, and mitomycin C (**Figure 5F**).

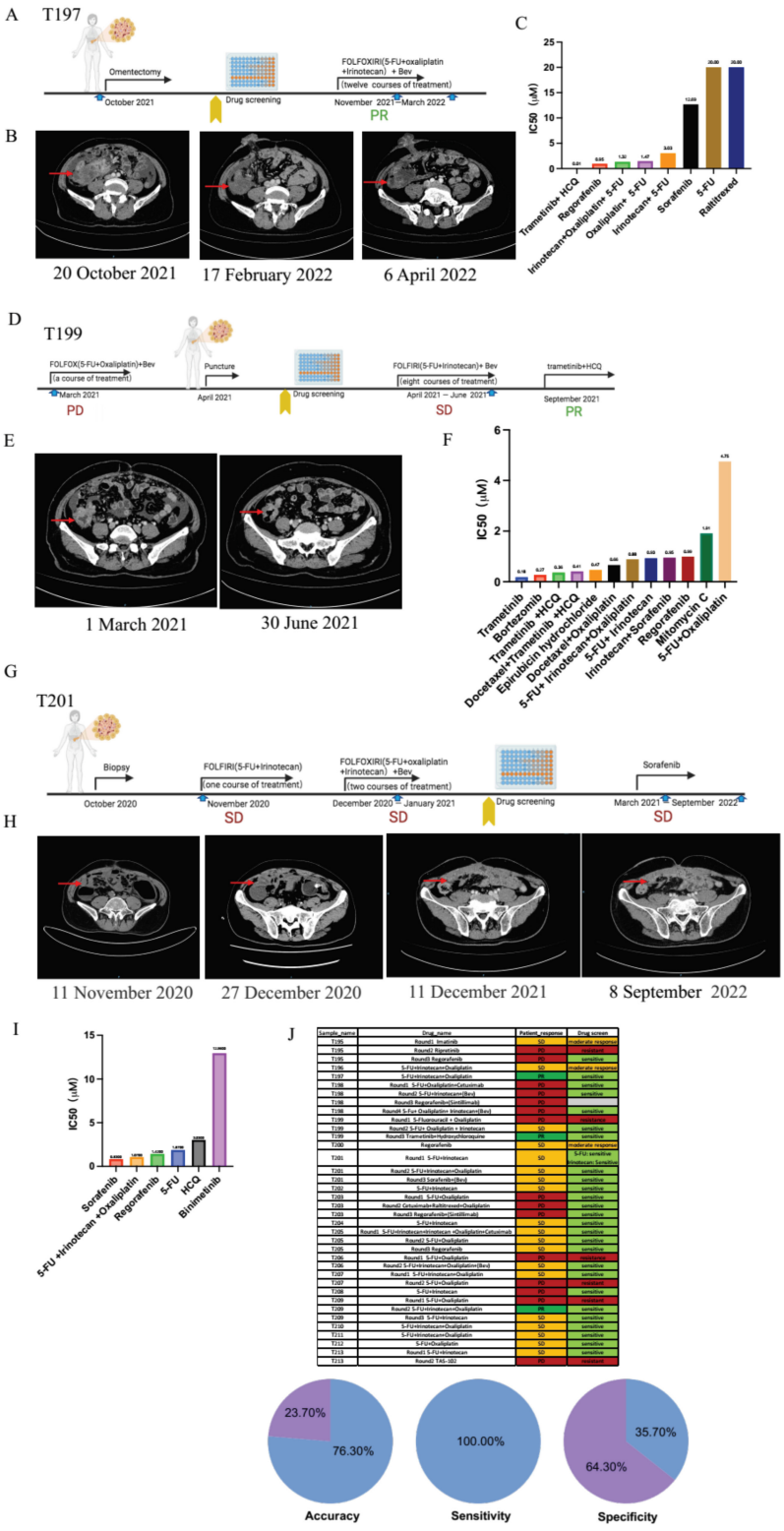


Figure 5. PDOs retain the previous treatment responses of colorectal cancer patients. **A.** Treatment procedure and responses of patient T197 from surgery. Each 9 round of treatment received by the patient is displayed here. The blue arrow tips indicate the images taking time points in (B). PR indicates partial response. **B.** Tumor CT scan images show that the ileocecal region and cecum of patient T197 continued to diminish during the clinical treatment. The red arrows indicate tumors. **C.** IC50 values of various drugs for PDO197. **D.** Treatment procedure and responses of patient T199 from surgery. Each round of treatment received by the patient is displayed here. The blue arrow tips indicate the images taking time points in (E). PD indicates disease. SD indicates stable disease. **E.** Tumor CT scan images show that the ileocecal region of patient T199 continued to diminish during the clinical treatment. The red arrows indicate tumors. **F.** IC50 values of various drugs for PDO199. **G.** Treatment procedure and responses of patient T201 from surgery. Each round of treatment received by the patient is displayed here. The blue arrow tips indicate the images taking time points in (H). SD indicates stable disease. **H.** Tumor CT scan images show that the intestinal canal metastases of patient T201 continued to diminish during the clinical treatment. The red arrows indicate tumors. **I.** IC50 values of various drugs for PDO201. **J.** Drug screening results of colorectal cancer organoids matching the patients' previous treatment outcomes. The laboratory on the right shows the clinical outcomes of the patients (19 patient cases) and the organoid responses of the drugs that the patients received in each round of treatment. The bottom graph shows accuracy, sensitivity, and specificity of drug screening results matching the patients' previous treatment outcomes.

Patient T201 was diagnosed at the IV stage, and the location of the lesion was ileocecal with peritoneal metastasis. The patient sequentially underwent surgical biopsy, adjuvant chemotherapy (5-FU, irinotecan, oxaliplatin), and antibody therapy (bevacizumab). Three months after treatment, the patient's condition was stabilized (**Figure 5G**). The lesion in the gyrus had little change and the tumor was stable, as shown in **Figure 5H**. We derived organoids (PDO201) from the colon tumor tissue of this patient and conducted drug screening during these treatments. Our pharmaco-phenotyping results showed that PDO201 was sensitive to some drugs, including sorafenib, 5-FU+irinotecan+oxaliplatin, regorafenib, 5-FU, and HCQ. And it was resistant to the binimetinib drug (**Figure 5I**). After drug screening, the patient was treated with sorafenib for two years and maintained a stable condition.

The clinical outcomes of the 19 patients and their corresponding PDO pharmaco-phenotyping results are summarized in **Figure 5J**. Notably, 71.43% of the treatments, which include at least one drug that was tested to be sensitive by PDOs, achieved stable disease or partial response. Conversely, 100% of the treatments, which do not include any drug that was tested to be sensitive or moderately responsive by PDOs, developed progressive disease. Thus, the PDO pharmaco-phenotyping results are highly correlated with clinical outcomes, with 76.30% accuracy. Thus, the PDO pharmaco-phenotyping results are highly correlated with clinical outcomes ($p = 0.00108207$), with 0.50964719 correlation coefficient and 44.94% AUC, 76.30% accuracy, 100% sensitivity, and 35.7% specificity.

Some inconsistent cases were observed in our studies. For instance, patient T199 showed resistance to the combined treatment: 1) 5-FU+irinotecan and 2) 5-FU+irinotecano+Oxaliplatin, while our pharmaco-phenotyping results indicated that PDO199 was sensitive to these treatments. Ultimately, the patient developed progressive disease (**Supplemental Figure 5**). The inconsistency between treatment response and pharmaco-phenotyping results could be attributed to the absence of the tumor microenvironment of PDO or tumor evolution. Overall, our PDO chemosensitivity profile was largely consistent with the retrospective clinical data from these patients.

PDO mutated pharmaco-phenotyping predicates patient-specific sensitivities for personalized therapy

Over the past decade, next-generation sequencing has been extensively utilized in precision oncology, making significant progress in aligning targeted therapies with predictive gene signatures. Subsequently, we performed genomics sequencing for tumors in several patients, primarily focused on metastatic colorectal cancers. Patient T206 was resistant to 5-FU and oxaliplatin treatment and was diagnosed at the IV stage with peritoneal metastasis in June 2020 (**Figure 6A**).

Notably, the tumor was resistant to three rounds of treatment before cytoreductive surgery (CRS) on 29 March 2021 (**Figure 6A**). Targeted DNA sequencing revealed the presence of *SMAD4* and *TP53* mutations in her tumor (*SMAD4* was a missense mutation in SNV, and *TP53* was a splice site mutation in SNV). Meanwhile, we also generated organoids (PDO206) for drug screening, and identified several drug combinations, including 5-FU+irinotecan+oxaliplatin, which were sensitive, together with several other drug combinations, such as Binimetinib+cetuximab, 5-FU+oxaliplatin, encorafenib+ cetuximab, which were resistant to this patient (**Figure 6B**). Because 5-FU, irinotecan and oxaliplatin are therapeutic drugs commonly used for treating colorectal cancer patients at late stages, the patient was treated with 5-FU+irinotecan+oxaliplatin together with bevacizumab, which is a monoclonal antibody medication used to block VEGF, for six courses and then continued with capecitabine+bevacizumab. These combined treatments achieved effective tumor control (Figure 6C), and no recurrence or metastasis was observed during the follow-up period.

Patient T207 was diagnosed at the IV stage with peritoneal metastasis. Initial treatment involved a regimen of 5-FU + oxaliplatin + bevacizumab but resulted in progressive disease. Subsequently, the patient underwent a Miles surgery followed by an ablative hepatic resection (**Figure 6D**). We generated PDOs and performed drug screening, finding that the patient was sensitive to 5-FU + irinotecan + oxaliplatin, 5-FU + irinotecan, and mitomycin C, but resistant to 5-FU + oxaliplatin + cetuximab and 5-FU + oxaliplatin (**Figure 6E**). Whole genome exome sequencing revealed a *SMAD4* mutation (*SMAD4* deletion in CNV). After analyzing all the information, we focused on the treatment of the patient using 5-FU+irinotecan with the combination of surgeries. Ten months post the treatment, although the tumor was in stable disease status, we discovered that patient had abdominal wall metastasis and underwent abdominal wall tumor resection (**Figure 6D**). The patient was then continued to be treated with 5-FU+irinotecan and achieved stable disease (**Figure 6F**).

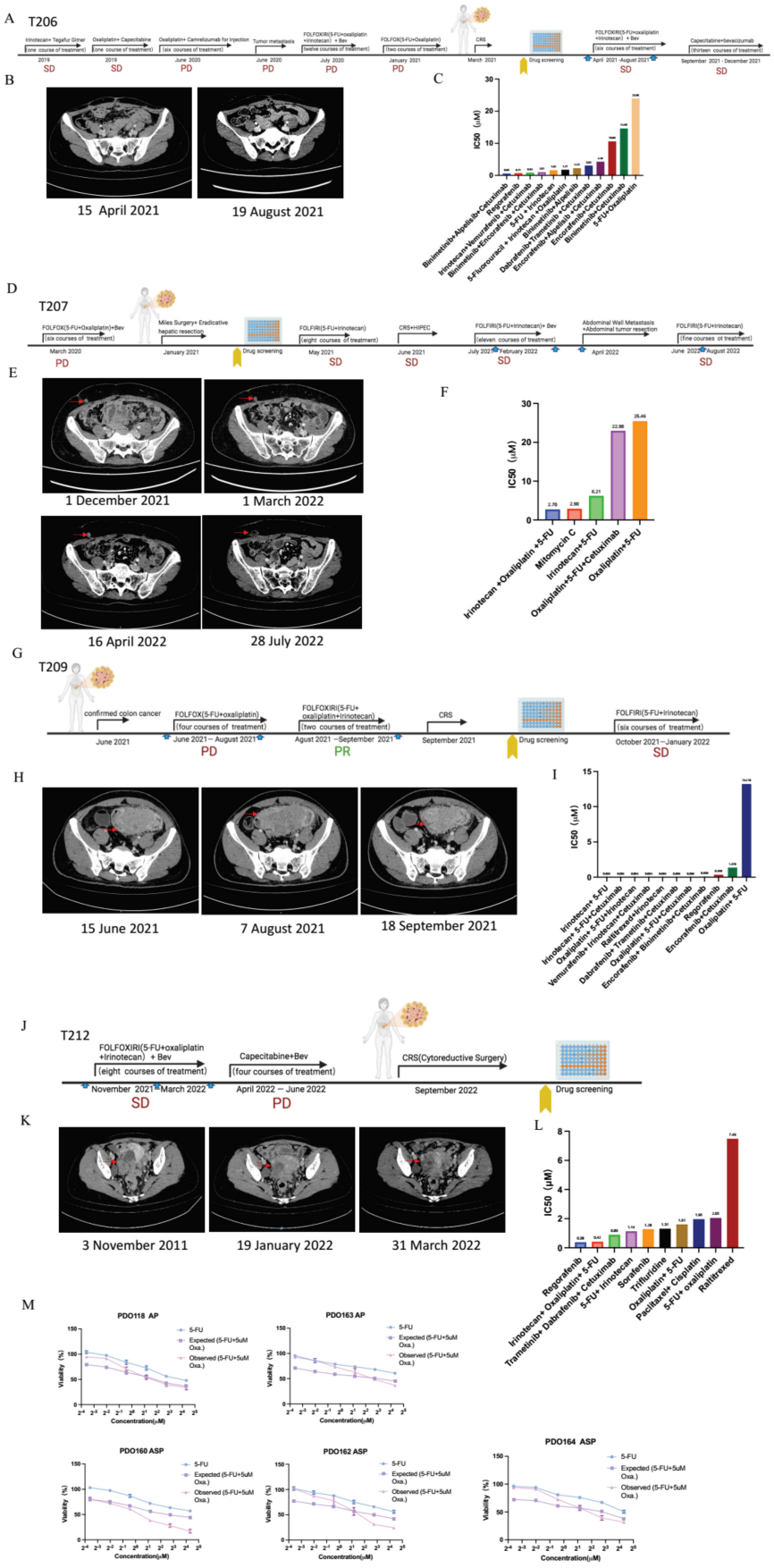


Figure 6. The PDO A/K/S/P mutated platform predicts personalized therapy for patients with colorectal cancer. A. Treatment procedure and responses of patient T206 from surgery. Each round of treatment received by the patient is displayed here. The blue arrow tips indicate the images taking time points in (B). PD indicates

disease. SD indicates stable disease. **B.** Tumor CT scan images show that no tumor recurrence or metastasis observed during the clinical treatment. **C.** IC50 values of various drugs for PDO206. **D.** Treatment procedure and responses of patient T207 from surgery. Each round of treatment received by the patient is displayed here. The blue arrow tips indicate the images taking time points in (E). PD indicates disease. SD indicates stable disease. **E.** Tumor CT scan images show that subcutaneous implantation metastasis on the lower right abdominal wall of patient T207 continued to diminish during the clinical treatment. The red arrows indicate tumors. **F.** IC50 values of various drugs for PDO207. **G.** Treatment procedure and responses of patient T209 from surgery. Each round of treatment received by the patient is displayed here. The blue arrow tips indicate the images taking time points in (H). PR indicates partial response. PD indicates disease. SD indicates stable disease. H. Tumor CT scan images show that peritoneum metastasis of patient T209 continued to diminish during the clinical treatment. The red arrows indicate tumors. **I.** IC50 values of various drugs for PDO209. **J.** Treatment procedure and responses of patient T212 from surgery. Each round of treatment received by the patient is displayed here. The blue arrow tips indicate the images taking time points in (K). PD indicates disease. SD indicates stable disease. **K.** Tumor CT scan images show that right ovary of patient T212 to decreased in size and then increased again during the clinical treatment. The red arrows indicate tumors. **L.** IC50 values of various drugs for PDO212. **M.** Drug response curves of PDO118, PDO163, PDO160, PDO164 and PDO162 treated with 5-FU alone, predicted additive curve, and 5-FU combined with IC20 oxaliplatin. The results are expressed as the mean ± S.E.M.

Table 2. T206, T207 and T209, all had SMAD4 mutations.

Name	Patient type	Sample name	Drug name	Patient response	Drug screening IC50	Drug screening	Type 3
Patient1	NA	T199	5-FU+Oxaliplatin	PD	14.75	Resistant	Consistent
Patient2	SP	T206	5-FU+Oxaliplatin	PD	23.95	Resistant	Consistent
Patient3	S	T207	5-FU+Oxaliplatin	PD	25.46	Resistant	Consistent
Patient4	ASP	T209	5-FU+Oxaliplatin	PD	13.21	Resistant	Consistent
Patient5	AP	T212	5-FU+Oxaliplatin	SD	2.05	Sensitive	Consistent

Patient T209 was diagnosed at stage IV with peritoneal metastasis in June 2021. He had a tumor in the proximal sigmoid colon with a thickened wall forming a mass. Initial treatment consisted of four cycles of 5-FU + oxaliplatin, but the disease progressed. He was subsequently treated with 5-FU + irinotecan + oxaliplatin and achieved a PR. The patient then underwent CRS (**Figure 6G**). We generated PDO209 and performed drug screening. We found that PDO209 was sensitive to most drug combinations but resistant to 5-FU+oxaliplatin (**Figure 6H**). Whole genome exome sequencing revealed a *SMAD4* mutation (*SMAD4* deletion in CNV). After analyzing all the information, we decided to treat the patient with 5-FU+ irinotecan combined with surgery and achieved stable disease **(Figure 6G)**.

Patient T212 was diagnosed at the IV stage with a lung and peritoneal metastasis. The patient has colon cancer located in the upper middle rectum, with thickening of the intestinal wall circumference. Prior to our drug screening, she was treated with chemotherapy (5-FU+oxaliplatin) and bevacizumab (**Figure 6J**). Imaging data revealed a gradual decrease in the thickness of her intestinal wall. After four months of treatment, she underwent four courses of capecitabine+bevacizumab, followed by CRS (**Figure 6K**). Organoid (PDO212) were established, and drug screening results indicated that regorafenib, 5-FU+irinotecan, 5-FU+oxaliplatin, sorafenib, trifluridine, 5-FU+irinotecan+oxaliplatin and paclitaxel+cisplatin could be potential candidates for this patient (**Figure 6L**). Whole genome exome sequencing revealed mutations in the *APC* and *TP53* genes (*APC* had a frame-shift insertion in SNV, while *TP53* had a deletion in CNV). The patient achieved stable disease. Conversely, patient T212, who did not have a SMAD4 mutation, demonstrated sensitivity to the 5FU+ oxaliplatin treatment in the organoid screening.

We present a summary of the key mutation data, organoid screening results, and corresponding clinical treatment statuses for four patients (**Figure 6, Table 2**). Our findings indicated that three patients, T206, T207 and T209, all had *SMAD4* mutations (**Table 2**). The organoid screening results for these patients showed resistance to the 5-FU+oxaliplatin treatment, which was consistent with disease progression clinically. Conversely, patient T212, who did not have a *SMAD4* mutation, demonstrated sensitivity to the 5-FU+oxaliplatin treatment in the organoid screening and exhibited stable clinical disease treatment (**Table 2**). These observations led us to hypothesize that the combination therapy of 5-FU+oxaliplatin may not be suitable for patients with *SMAD4* mutations. To further validate our hypothesis, we selected five PDOs for in vitro combination therapy and confirmed this phenomenon. Organoids without *SMAD4* mutations were sensitive to the combination therapy of 5-FU+Oxaliplatin, while those with *SMAD4* mutations showed no sensitivity to the combination therapy (**Figure 6M**). Therefore, our data suggest that the use of a combination of 5-FU+oxaliplatin should be minimized in patients with *SMAD4* mutations. For patients without *SMAD4* mutations, a combination of 5-FU and Oxaliplatin could be used to improve clinical treatment efficacy.

Discussion

The emergence of precision oncology has transformed the landscape of cancer therapy, enabling tailored treatment strategies based on the unique molecular characteristics of individual patients and tumors [20, 39, 40]. In our study, we investigated the utility of patient-derived organoids (PDOs) for guiding personalized therapy in colorectal cancer, focusing on key gene mutations implicated in

colorectal carcinogenesis. Our findings shed light on the complex interplay between genetic alterations and drug responses, paving the way for more effective and targeted interventions in this challenging disease.

PDOs represent a promising model system that faithfully recapitulates the heterogeneity and complexity of individual tumors [19, 26]. By culturing PDOs from tumor samples obtained during surgical resection or biopsy, this approach allows for high-throughput drug screening and detailed molecular profiling, offering valuable insights into tumor biology and options for personalized therapy [21, 22, 25]. In our previous study, we have used PDOs to predict the progression-free survival of patients with stage IV colorectal cancer [41]. In this study, we showed that PDOs derived from a different set of colorectal cancer samples harboring mutations in key drivers, such as *APC*, *KRAS*, *SMAD4*, and *TP53*, could serve as an invaluable resource for studying genotype-phenotype correlations and drug responses. The successful establishment and characterization of these PDOs underscored their potential as predictive tools for personalized treatment selection.

Our study revealed distinct patterns of drug sensitivity associated with specific genomic alterations in colorectal cancer. *TP53*, a critical tumor suppressor gene frequently mutated in colorectal cancer, plays a pivotal role in regulating cell cycle progression and apoptosis [42, 43]. Notably, we observed higher prevalence of *TP53* mutations in advanced stage tumors located in the sigmoid region, suggesting potential implications for regionalized treatment approaches. Notably, PDOs carrying mutations in *TP53* exhibited differential responses to chemotherapy agents commonly used in clinical practice. Our findings suggest that the mutational status of *TP53* may influence therapeutic outcomes, highlighting the importance of targeted interventions based on genomic profiling.

SMAD4 is a central mediator for the transforming growth factor beta (TGF-β) signalling and plays important roles in many biological processes, including cell growth, differentiation, apoptosis, migration, as well as cancer initiation and progression [44, 45]. *SMAD4* alterations are prevalent in advanced colorectal tumors and have been implicated in tumor progression and metastasis [46, 47]. PDOs with *SMAD4* mutations demonstrated altered responses to targeted therapies designed to modulate the TGF-β signaling pathway. We found that organoids without *SMAD4* mutations were more sensitive to the combination therapy of 5-FU+Oxaliplatin than those with *SMAD4* mutations. Therefore, our data suggest that the use of a combination of 5-FU+oxaliplatin should be minimized in patients with *SMAD4* mutations. For patients without *SMAD4* mutations, a combination of 5-FU and Oxaliplatin could be used to improve clinical treatment efficacy. Our results highlight the feasibility of leveraging PDOs to uncover genotype-specific drug responses, paving the way for personalized treatment strategies in *SMAD4*-mutated CRC.

APC mutations are early events in colorectal tumorigenesis and are implicated in the development of adenomatous polyps [2]. Our study elucidated the impact of *APC* mutations on drug sensitivity using PDOs, providing valuable data for optimizing therapeutic regimens tailored to *APC*-mutant CRC. PDOs carrying *APC* mutations displayed distinct responses to Wnt pathway inhibitors, emphasizing the potential for precision medicine approaches tailored to specific genetic alterations. These findings underscore the potential of PDO-based drug screening in guiding treatment decisions based on specific genomic alterations.

KRAS mutations are prevalent in CRC and are associated with resistance to certain targeted therapies [48, 49]. Our study corroborates previous findings indicating that *KRAS*-mutant PDOs exhibit limited sensitivity to EGFR-targeted therapies, underscoring the necessity for alternative treatment strategies in this molecularly defined subset [49, 50]. The use of PDOs enables precise evaluation of drug efficacy based on *KRAS* mutation status, facilitating informed clinical decision-making.

The integration of PDO-based drug screening into clinical decision-making holds immense promise for enhancing treatment outcomes in colorectal cancer patients [39, 40]. Looking ahead, the widespread adoption of PDO technology in routine clinical practice necessitates overcoming several logistical and technical challenges. Standardization of PDO culture protocols, scalability for high-throughput screening, and validation of predictive biomarkers are critical steps towards establishing PDO-based assays as integral components of personalized cancer care pathways [51]. Furthermore, ongoing efforts to elucidate the functional consequences of genomic alterations and their interplay with the tumor microenvironment will deepen our understanding of therapeutic vulnerabilities and resistance mechanisms in colorectal cancer.

In summary, our study underscores the transformative potential of PDOs in guiding personalized therapy for colorectal cancer. By elucidating the intricate relationship between genetic mutations and drug responses, we provide a roadmap for the development of tailored treatment strategies that prioritize patient-centric care and optimize clinical outcomes. Moving forward, the integration of

PDO-based pharmacogenomic profiling into clinical trials and routine practice holds great promise for advancing precision oncology and improving the lives of patients with colorectal cancer.

Materials and Methods

Sample collection and clinical case studies

Fresh tumor biopsies and paired blood samples pathologically diagnosed with CRC were collected from two hospitals in China. One hospital was the Kiang Wu Hospital, Macau from August 2016 to December 2022. Another hospital was the Sixth Affiliated Hospital of Sun Yat-sen University (Accreditation number: 2021ZSLYEC-117). Prior patient written consents were obtained from donors by informing them of the use for genomic sequencing, organoid culture, drug test, publication, and associated scientific studies. All collected tumors were further confirmed, classified, and stage assessed through TNM staging. All collected tumors were further confirmed, classified, and stage assessed through TNM staging. The protocol of this study was assessed and approved by the ethics committees of University of Macau, Kiang Wu Hospital and Six Affiliated Hospital of Sun Yat-sen University. Detailed clinicopathological characteristics of all CRC patients included in this study are summarized in Supplemental Data 1, the prior consents to publish information of gender, age, ethnicity and associated clinical characteristics were obtained from subjects.

Clinical trials guided by PDO mutated Pharmaco-phenotyping were intended to be clinical case studies. The trials were assessed and approved by the ethics committees of the hospitals. All patients provided written informed consent per the principles of the Declaration of Helsinki.

Tissue dissociation

Upon arrival, the tumor tissues were firstly minced into 1–3 mm^3 pieces. Two random pieces were picked up for DNA isolation and formalin fixing. The remaining portions were digested with digestion buffer (**Supplemental Data file3**) at 37 °C for 0.5-1h with gentle shaking until the visible pieces disappeared, and then centrifuged at 2000 rpm for 3 min, washed with DMEM supplemented with 10% FBS, and spun down again at 2000 rpm for 3 min. If the pellet showed a visible red color, erythrolysis was performed with RBC lysis buffer (eBiosciences) before the washing step. The remaining tumor cells were collected for organoid culture and cryopreservation.

Organoid culture and passage

Dissociated tumor cells were resuspended in Matrigel (Corning) solution, then seeded in prewarmed culture plates at 31 μL per drop. Once cell Matrigel drops were solidified at 37 °C, 2.5 ml/well organoid culture medium was added in to initiate continuous culture. Medium was refreshed every 2~3 days and passage passages were performed every 5~10 days depending on organoid density and size.

After removal of the culture medium, the organoids were resuspended in cold 0.25% trypsin by pipetting, later were transferred to 37 °C for 2min allowing further dissociation to smaller cell aggregates. Additional pipetting and incubation were performed as required. The cells were then spun down at 2000 rpm for 3 minutes, washed with 5 mL DMEM and spun down again. The cells were resuspended in Matrigel at a 1:3 ratio, seeded into the plates and cultured as described above.

There was no significant difference in the longest time or in the number of passages between the organoids derived from cryopreserved or fresh tissue. There were also no differences in organoids between different mutation types. A large proportion of the organoids were used for drug testing because the authors needed to complete the drug screening in a short time. Authors had enough PDOs to perform different types of experiments in only a few cases. Therefore, the authors had to establish a priority order based on the PDOs, which was: 1) drug sensitive test; 2) RNA-sequense; 3) frozen; 4) DNA-seq; 5) continuing passaging; 6) histological study; etc.

Histology, immunostaining and *immunofluorescence*

Tumor tissues and organoids were fixed in 10% formalin. This was followed by gradient dehydration, wax immersion, paraffin embedding and sectioning. Fixed organoids were stained with haematoxylin prior to dehydration and paraffin embedding. Haematoxylin and eosin (HE) staining, immunostaining and immunofluorescence were performed on 5 μm sections using standard protocols (44,45). The antibodies used were listed as following: Ki-67 (CST, 9449S, 1:500), Ki67 (1:400, CST, 9449 S), β − C*at* enin (Santa Cruz, sc-59737), CK7 (abcam, ab181598), CK20 (abcam, ab854). All images were captured on a Nikon microscope (Nikon, ECLIPSE, Ci).

DNA and RNA extraction

Of 148 samples assigned for WES, DNA of 134 samples were isolated from bulk fresh primary tumors, 14 from microdissected formalin fixed, paraffin embedded (FFPE) samples. According to the manufacturer's instructions, genomic DNA and paired blood were extracted using the DNeasy Blood &

Tissue Kit (Qiagen). LASER-capture microdissection of FFPE samples was performed using the Leica LMD 7000 Laser Micro Dissection System so that clusters of tumor cells and adjacent normal tissue could be separately dissected for genomic DNA preparation using the QIAamp DNA Micro Kit (Qiagen). RNA was extracted from the organoids using the RNeasy Micro Kit (Qiagen).

Whole exome sequencing

After sonication using a hydrodynamic shearing system (Covaris, M220, USA) to generate 180-280 bp fragments, a total of 1 μg genomic DNA per sample was used for library preparation. Whole exome capture libraries were prepared using the Agilent Sure Select Target Enrichment Kit (Agilent Technologies, CA, USA) according to their protocols. The libraries were clustered using Nova Seq S4 reagent kit (Illumina, San Diego, USA) on a cBot Cluster Generation System and sequenced using Illumina Nova Seq 6000. This sequencing was performed by Beijing Youji Technology Co., Ltd.

Whole-exome sequencing data analysis

Quality control of the DNA-sequencing data was carried out using MultiQC (v1.11). Adapter trimming was performed using Trim Galore (v0.6.7). Sequence reads were aligned to human genome build 38 (Hg38) using Burrows-Wheeler Alignment tool with maximal exact matches (v0.7.17) [52] followed by reducing duplicates with Sambamba (v0.6.6) [53], realignment of indels and base recalibration with Genome Analysis Tool Kit (v4.2.2.0) [54] according to the best practice guidelines.

Somatic SNVs were called by three independent programs with default parameters, including MuTect2 (v4.2.2.0) [55], Strelka2 (v2.9.2) [56], and LANCET (v1.1.0) [57]. Paired blood control or adjacent control samples were applied as the reference to call somatic mutations of each tumor or PDO independently. The results of each caller were stored in VCF format and further filtered for PASS variants. The vcf2maf tools (https://github.com/mskcc/vcf2maf) was used to convert VCF into MAF with performing annotation by ENSEMBL Variant Effect Predictor according to reference release 104 [58]. Only mutations detected by at least two callers were kept as true positive ones and assigned for further analysis. To detect somatic CNAs (copy number alterations), BAM files were analyzed using CNV kit (v0.9.9) [59] and Sequenza (v3.0.0) [60] by comparing tumors or PDO to reference blood control or adjacent control samples.

RNA sequencing

RNA libraries were prepared using NEB Next Ultra Directional RNA Library Prep kit for Illumina (NEB) following the manufacturer's protocol. This sequencing performed by Novo gene Co., Ltd.

RNA sequencing analysis

RNA sequencing was performed for 17 PDOs and the quality check was carried out using MultiQC (v1.11) [61]. RNA reads were aligned to human reference genome GRCh38 using HISAT2 (2.2.1) [62] followed by counting RNA reads by feature Counts (2.0.1) [63], one of programs in Subread package. Genes with zero read counts for all samples were removed. Then differentially expressed genes were identified using DESeq2 [64]. The cutoff criteria for DESeq2 were the absolute value of log2 fold change > 1, p-value < 0.05, FDR (p adj) value < 0.05. The multiple hypothesis testing was performed using Benjamin–Hochberg correction implemented in the DESeq2. Gene Ontology (GO) terms analysis was performed by Metascape [65], results were filtered by absolute p-value < 0.05, and FDR value < 0.05.

Drug screening

We organized a drug library 47 drugs on CRC, including 18 chemotherapy drugs and 29 target drugs (Supplemental Data file2). Compounds were dissolved in DMSO at the concentration of 10 mM and then in sterile PBS and added in 384-well plates at 6-point serial dilutions (0.82–200 μM, as 10× working dilution). Initially, organoids were enzymatically dissociated into single cells, then diluted with the medium for drug screening (Y-27632, SB202190, and A83-01 were removed from the complete culture medium). For drug response assay, the organoids were supplemented with 2.5% Matrigel and seeded in type-I collagen gel precoated 384-well plate at a density of about 3,500 cells per well. The third day, drugs were added into each well at 6-point serial dilutions (0.12–300 μM) and incubated for 4 days. The organoid viability was examined with the Cell Titer-Lumi TM Plus assay (Beyotime). IC50 values were calculated using GraphPad 9.0 Prism software, with luminescence readings from drug-treated wells normalized to control wells and expressed as percentage cell viability.

Evaluation of clinical outcomes

The clinical response of patients in this treatment in this study was assessed by computed tomography (CT) or magnetic resonance imaging (MRI) according to Response Evaluation Criteria in Solid Tumors (RECIST) version 1.1, as follows complete response (CR), partial response (PR), stable disease (SD) and progressive disease (PD). CR and PR indicated that the treatments had a good response in patients [66]. For

patients with incurable locally advanced or metastatic colorectal cancer, the primary goal of clinical treatment was to improve survival and maintain quality of life, and SD results were acceptable. The Common Terminology Criteria for Adverse Event (CTCAE) version 4.0 has been used to assess the toxicity of drug treatments.

Statistics and reproductivity

All representative experiments were performed in triplicates or duplicates independently. The results were reported as the mean ± SEM or mean ± SD. Statistical significance was calculated using the two-sided t test, unless otherwise indicated. The p values were considered statistically significant if the p-value ≤ 0.05.

Supplementary Material

Supplementary data file 1, clinical information.
https://www.ijbs.com/v23p0358s1.pdf
Supplementary data file 2, figures.
https://www.ijbs.com/v23p0358s2.pdf
Supplementary data file 3.
https://www.ijbs.com/v23p0358s3.pdf

Acknowledgements

The authors thank members of Dr. Deng's laboratory for helpful discussion and technical assistance. We thank all patients and their families for participating in this study.

Funding

This work was financially supported by the Science and Technology Development Fund, Macau SAR (0009/2022/AKP, 0054/2023/RIA1, and 0129/2024/RIA2).

Data availability statement

The raw data supporting the findings of this study are available within the article and its Supplemental information files or from the corresponding author upon reasonable request.

Author contributions

Jinghong Chen, Jing-Bo Zhou, and Fangyuan Shao conducted the experiments, performed data analysis, and wrote the manuscript, contributing equally to this work. Yangyang Feng and Xiangpeng Chu assisted with the data analysis. Ling Li, Kai Miao, Duo Liu, Weihao Deng, Wen-Li Zhu, Guang-Hui Luo, and Kin-Iong Chan contributed to data collection. Zheyu Cai, Jinbao Liu provided project advice, and Chu-xia Deng, Jian Cai, and Fangyuan Shao designed and supervised the project, as well as revised the manuscript.

Consent to participate

Written informed consent was obtained from all individual participants included in the study.

Ethics approval

This study was approved by the Ethics Committee of Centro Hospitalar Conde de S. Januário (Accreditation number: BSERE16-APP010-FHS). All procedures performed were in accordance with the ethical standards of the institutional research committee and with the 1964 Helsinki declaration and its later amendments.

Human ethics and consent to participate declarations

This study received ethical approval as stated above, and all participants provided informed consent.

Competing Interests

The authors have declared that no competing interest exists.

References

1. Bray F, Laversanne M, Sung H, Ferlay J, Siegel RL, Soerjomataram I, et al. Global cancer statistics 2022: GLOBOCAN estimates of incidence and mortality worldwide for 36 cancers in 185 countries. CA Cancer J Clin. 2024; 74: 229-63.
2. Kinzler KW, Vogelstein B. Lessons from hereditary colorectal cancer. Cell. 1996; 87: 159-70.
3. Pinto D, Clevers H. Wnt, stem cells and cancer in the intestine. Biol Cell. 2005; 97: 185-96.
4. Budagyan K, Cannon AC, Chatoff A, Benton D, Kurimchak AM, Araiza-Olivera D, et al. KRAS G12V mutation-selective requirement for ACSS2 in colorectal adenoma formation. Cell Rep. 2025; 44: 115444.
5. Hasbullah HH, Musa M. Gene Therapy Targeting p53 and KRAS for Colorectal Cancer Treatment: A Myth or the Way Forward? Int J Mol Sci. 2021; 22.
6. Yu X, Li Z, Yu J, Chan MT, Wu WK. MicroRNAs predict and modulate responses to chemotherapy in colorectal cancer. Cell Prolif. 2015; 48: 503-10.
7. Lee WS, Yun SH, Chun HK, Lee WY, Yun HR, Kim J, et al. Pulmonary resection for metastases from colorectal cancer: prognostic factors and survival. Int J Colorectal Dis. 2007; 22: 699-704.
8. Van Cutsem E, Nordlinger B, Adam R, Kohne CH, Pozzo C, Poston G, et al. Towards a pan-European consensus on the treatment of patients with colorectal liver metastases. Eur J Cancer. 2006; 42: 2212-21.
9. Yoo PS, Lopez-Soler RI, Longo WE, Cha CH. Liver resection for metastatic colorectal cancer in the age of neoadjuvant chemotherapy and bevacizumab. Clin Colorectal Cancer. 2006; 6: 202-7.
10. Mosele MF, Westphalen CB, Stenzinger A, Barlesi F, Bayle A, Bieche I, et al. Recommendations for the use of next-generation sequencing (NGS) for patients with advanced cancer in 2024: a report from the ESMO Precision Medicine Working Group. Ann Oncol. 2024; 35: 588-606.
11. Gibbs SN, Peneva D, Cuyun Carter G, Palomares MR, Thakkar S, Hall DW, et al. Comprehensive Review on the Clinical Impact of Next-Generation Sequencing Tests for the Management of Advanced Cancer. JCO Precis Oncol. 2023; 7: e2200715.
12. Chakravarty D, Solit DB. Clinical cancer genomic profiling. Nat Rev Genet. 2021; 22: 483-501.
13. Avci CB, Bagca BG, Shademan B, Takanlou LS, Takanlou MS, Nourazarian A. Precision oncology: Using cancer genomics for targeted therapy advancements. Biochim Biophys Acta Rev Cancer. 2025; 1880: 189250.
14. Cheng WC, Chung IF, Chen CY, Sun HJ, Fen JJ, Tang WC, et al. DriverDB: an exome sequencing database for cancer driver gene identification. Nucleic Acids Res. 2014; 42: D1048-54.
15. Arnedos M, Vicier C, Loi S, Lefebvre C, Michiels S, Bonnefoi H, et al. Precision medicine for metastatic breast cancer--limitations and solutions. Nat Rev Clin Oncol. 2015; 12: 693-704.

16. Hill SJ, Decker B, Roberts EA, Horowitz NS, Muto MG, Worley MJ, Jr., et al. Prediction of DNA Repair Inhibitor Response in Short-Term Patient-Derived Ovarian Cancer Organoids. Cancer Discov. 2018; 8: 1404-21.
17. Stratton MR, Campbell PJ, Futreal PA. The cancer genome. Nature. 2009; 458: 719-24.
18. Holohan C, Van Schaeybroeck S, Longley DB, Johnston PG. Cancer drug resistance: an evolving paradigm. Nat Rev Cancer. 2013; 13: 714-26.
19. Neal JT, Li X, Zhu J, Giangarra V, Grzeskowiak CL, Ju J, et al. Organoid Modeling of the Tumor Immune Microenvironment. Cell. 2018; 175: 1972-88 e16.
20. Han X, Cai C, Deng W, Shi Y, Li L, Wang C, et al. Landscape of human organoids: Ideal model in clinics and research. Innovation (Camb). 2024; 5: 100620.
21. Xue W, Wang T, Yao J, Wu W, Chen D, Yan B, et al. Use of patient-derived tumor organoid platform to predict the benefit of postoperative adjuvant chemotherapy for poor responders to neoadjuvant chemoradiotherapy in locally advanced rectal cancer. Bioeng Transl Med. 2023; 8: e10586.
22. Chen P, Zhang X, Ding R, Yang L, Lyu X, Zeng J, et al. Patient-Derived Organoids Can Guide Personalized-Therapies for Patients with Advanced Breast Cancer. Adv Sci (Weinh). 2021; 8: e2101176.
23. Ding RB, Chen P, Rajendran BK, Lyu X, Wang H, Bao J, et al. Molecular landscape and subtype-specific therapeutic response of nasopharyngeal carcinoma revealed by integrative pharmacogenomics. Nat Commun. 2021; 12: 3046.
24. Shao F, Lyu X, Miao K, Xie L, Wang H, Xiao H, et al. Enhanced Protein Damage Clearance Induces Broad Drug Resistance in Multitype of Cancers Revealed by an Evolution Drug-Resistant Model and Genome-Wide siRNA Screening. Adv Sci (Weinh). 2020; 7: 2001914.
25. Yao Y, Xu X, Yang L, Zhu J, Wan J, Shen L, et al. Patient-Derived Organoids Predict Chemoradiation Responses of Locally Advanced Rectal Cancer. Cell Stem Cell. 2020; 26: 17-26 e6.
26. Lee SH, Hu W, Matulay JT, Silva MV, Owczarek TB, Kim K, et al. Tumor Evolution and Drug Response in Patient-Derived Organoid Models of Bladder Cancer. Cell. 2018; 173: 515-28 e17.
27. Lee CS, Song IH, Lee A, Kang J, Lee YS, Lee IK, et al. Enhancing the landscape of colorectal cancer using targeted deep sequencing. Sci Rep. 2021; 11: 8154.
28. Yu J, Wu WK, Li X, He J, Li XX, Ng SS, et al. Novel recurrently mutated genes and a prognostic mutation signature in colorectal cancer. Gut. 2015; 64: 636-45.
29. Cancer Genome Atlas N. Comprehensive molecular characterization of human colon and rectal cancer. Nature. 2012; 487: 330-7.
30. van de Wetering M, Francies HE, Francis JM, Bounova G, Iorio F, Pronk A, et al. Prospective derivation of a living organoid biobank of colorectal cancer patients. Cell. 2015; 161: 933-45.
31. Brannon AR, Vakiani E, Sylvester BE, Scott SN, McDermott G, Shah RH, et al. Comparative sequencing analysis reveals high genomic concordance between matched primary and metastatic colorectal cancer lesions. Genome Biol. 2014; 15: 454.
32. Borras E, San Lucas FA, Chang K, Zhou R, Masand G, Fowler J, et al. Genomic Landscape of Colorectal Mucosa and Adenomas. Cancer Prev Res (Phila). 2016; 9: 417-27.
33. Baker SJ, Preisinger AC, Jessup JM, Paraskeva C, Markowitz S, Willson JK, et al. p53 gene mutations occur in combination with 17p allelic deletions as late events in colorectal tumorigenesis. Cancer Res. 1990; 50: 7717-22.
34. Wade M, Li YC, Wahl GM. MDM2, MDMX and p53 in oncogenesis and cancer therapy. Nat Rev Cancer. 2013; 13: 83-96.
35. Fujii M, Shimokawa M, Date S, Takano A, Matano M, Nanki K, et al. A Colorectal Tumor Organoid Library Demonstrates Progressive Loss of Niche Factor Requirements during Tumorigenesis. Cell Stem Cell. 2016; 18: 827-38.
36. Vassilev LT, Vu BT, Graves B, Carvajal D, Podlaski F, Filipovic Z, et al. In vivo activation of the p53 pathway by small-molecule antagonists of MDM2. Science. 2004; 303: 844-8.
37. Li W, Qiu T, Zhi W, Shi S, Zou S, Ling Y, et al. Colorectal carcinomas with KRAS codon 12 mutation are associated with more advanced tumor stages. BMC Cancer. 2015; 15: 340.
38. Li ZZ, Bai L, Wang F, Zhang ZC, Wang F, Zeng ZL, et al. Comparison of KRAS mutation status between primary tumor and metastasis in Chinese colorectal cancer patients. Med Oncol. 2016; 33: 71.
39. Singh M, Morris VK, Bandey IN, Hong DS, Kopetz S. Advancements in combining targeted therapy and immunotherapy for colorectal cancer. Trends Cancer. 2024; 10: 598-609.
40. Dosunmu GT, Shergill A. Colorectal Cancer: Genetic Underpinning and Molecular Therapeutics for Precision Medicine. Genes (Basel). 2024; 15.
41. Wang T, Tang Y, Pan W, Yan B, Hao Y, Zeng Y, et al. Patient-Derived Tumor Organoids Can Predict the Progression-Free Survival of Patients With Stage IV Colorectal Cancer After Surgery. Dis Colon Rectum. 2023; 66: 733-43.
42. Yan H, Jiang F, Yang J. Association of beta-Catenin, APC, SMAD3/4, Tp53, and Cyclin D1 Genes in Colorectal Cancer: A Systematic Review and Meta-Analysis. Genet Res (Camb). 2022; 2022: 5338956.
43. Kadioglu O, Saeed M, Mahmoud N, Azawi S, Mrasek K, Liehr T, et al. Identification of potential novel drug resistance mechanisms by genomic and transcriptomic profiling of colon cancer cells with p53 deletion. Arch Toxicol. 2021; 95: 959-74.
44. Zhao M, Mishra L, Deng CX. The role of TGF-beta/SMAD4 signaling in cancer. Int J Biol Sci. 2018; 14: 111-23.
45. Wang RH, Li C, Xu X, Zheng Y, Xiao C, Zerfas P, et al. A role of SMAD4 in iron metabolism through the positive regulation of hepcidin expression. Cell Metab. 2005; 2: 399-409.
46. Loevenich LP, Tschurtschenthaler M, Rokavec M, Silva MG, Jesinghaus M, Kirchner T, et al. SMAD4 Loss Induces c-MYC-Mediated NLE1 Upregulation to Support Protein Biosynthesis, Colorectal Cancer Growth, and Metastasis. Cancer Res. 2022; 82: 4604-23.
47. Waldner MJ, Neurath MF. TGFbeta and the Tumor Microenvironment in Colorectal Cancer. Cells. 2023; 12.
48. Bos JL. ras oncogenes in human cancer: a review. Cancer Res. 1989; 49: 4682-9.
49. Serna-Blasco R, Sanz-Alvarez M, Aguilera O, Garcia-Foncillas J. Targeting the RAS-dependent chemoresistance: The Warburg connection. Semin Cancer Biol. 2019; 54: 80-90.
50. Singh VK, Makhlouf Y, Sarker MMK, Craig S, Baena J, Greene C, et al. KRASFormer: a fully vision transformer-based framework for predictingKRASgene mutations in histopathological images of colorectal cancer. Biomed Phys Eng Express. 2024; 10.
51. Lin H, Wang Y, Cheng C, Qian Y, Hao J, Zhang Z, et al. Standard: Human intestinal cancer organoids. Cell Regen. 2023; 12: 24.
52. Li H, Durbin R. Fast and accurate long-read alignment with Burrows-Wheeler transform. Bioinformatics. 2010; 26: 589-95.
53. Tarasov A, Vilella AJ, Cuppen E, Nijman IJ, Prins P. Sambamba: fast processing of NGS alignment formats. Bioinformatics. 2015; 31: 2032-4.
54. McKenna A, Hanna M, Banks E, Sivachenko A, Cibulskis K, Kernytsky A, et al. The Genome Analysis Toolkit: a MapReduce framework for analyzing next-generation DNA sequencing data. Genome Res. 2010; 20: 1297-303.
55. McKenna A, Hanna M, Banks E, Sivachenko A, Cibulskis K, Kernytsky A, et al. The Genome Analysis Toolkit: a MapReduce framework for analyzing next-generation DNA sequencing data. 2010; 20: 1297-303.
56. Kim S, Scheffler K, Halpern AL, Bekritsky MA, Noh E, Källberg M, et al. Strelka2: fast and accurate calling of germline and somatic variants. 2018; 15: 591-4.
57. Narzisi G, Corvelo A, Arora K, Bergmann EA, Shah M, Musunuri R, et al. Genome-wide somatic variant calling using localized colored de Bruijn graphs. Communications biology. 2018; 1: 20.
58. McLaren W, Gil L, Hunt SE, Riat HS, Ritchie GR, Thormann A, et al. The ensembl variant effect predictor. 2016; 17: 1-14.
59. Talevich E, Shain AH, Botton T, Bastian BCJPcb. CNVkit: genome-wide copy number detection and visualization from targeted DNA sequencing. 2016; 12: e1004873.
60. Favero F, Joshi T, Marquard AM, Birkbak NJ, Krzystanek M, Li Q, et al. Sequenza: allele-specific copy number and mutation profiles from tumor sequencing data. 2015; 26: 64-70.
61. Ewels P, Magnusson M, Lundin S, Käller MJB. MultiQC: summarize analysis results for multiple tools and samples in a single report. 2016; 32: 3047-8.
62. Kim D, Langmead B, Salzberg SLJNm. HISAT: a fast spliced aligner with low memory requirements. 2015; 12: 357-60.
63. Liao Y, Smyth GK, Shi WJB. featureCounts: an efficient general purpose program for assigning sequence reads to genomic features. 2014; 30: 923-30.
64. Love MI, Huber W, Anders SJGb. Moderated estimation of fold change and dispersion for RNA-seq data with DESeq2. 2014; 15: 1-21.
65. Zhou Y, Zhou B, Pache L, Chang M, Khodabakhshi AH, Tanaseichuk O, et al. Metascape provides a biologist-oriented resource for the analysis of systems-level datasets. 2019; 10: 1523.
66. Eisenhauer EA, Therasse P, Bogaerts J, Schwartz LH, Sargent D, Ford R, et al. New response evaluation criteria in solid tumours: revised RECIST guideline (version 1.1). Eur J Cancer. 2009; 45: 228-47.